



Contribution to the Symposium: '6th Zooplankton Production Symposium'

Original Article

Reassessment of the life cycle of the pteropod *Limacina helicina* from a high resolution interannual time series in the temperate North Pacific

Kang Wang^{1,2,†}, Brian P. V. Hunt^{1,2,3*,†}, Cui Liang⁴, Daniel Pauly³, and Evgeny A. Pakhomov^{2,3}

¹Hakai Institute, PO Box 309, Heriot Bay, BC V0P 1H0, Canada

²Department of Earth, Ocean and Atmospheric Sciences, University of British Columbia, 2207-2020 Main Mall, Vancouver, BC V6T 1Z4, Canada

³Institute for the Oceans and Fisheries, AERL, University of British Columbia, 231-2202 Main Mall, Vancouver, BC V6T 1Z4, Canada

⁴College of Ocean and Earth Sciences, Xiamen University, Xiamen, Fujian Province 361102, China

*Corresponding author: e-mail: b.hunt@oceans.ubc.ca.

†K. Wang and B. P. V. Hunt contributed equally to this work as joint first authors.

Wang, K., Hunt, B. P. V., Liang, C., Pauly, D., and Pakhomov, E. A. Reassessment of the life cycle of the pteropod *Limacina helicina* from a high resolution interannual time series in the temperate North Pacific. – ICES Journal of Marine Science, 74: 1906–1920.

Received 18 August 2016; revised 11 January 2017; accepted 19 January 2017; advance access publication 11 April 2017.

Limacina helicina is the dominant pelagic gastropod mollusc species in temperate and polar ecosystems, where it contributes significantly to food webs and vertical flux. Currently, considerable uncertainty exists in the interpretation of *L. helicina*'s life cycle, hindering our understanding of its potential responses to environmental change. Here, we present size-frequency data on *L. helicina* collected from three consecutive years (2008–2010) in a North Pacific temperate fjord. Two methods of length-frequency analysis were used to infer the growth of *L. helicina*, i.e. linking successive means extracted from finite-mixture distributions, and using the ELEFAN software to fit seasonally oscillating versions of the von Bertalanffy growth equation to the available length-frequency data. Against a background of continuous low level spawning between spring and autumn, both approaches identified two sets of major cohorts, i.e. (i) spring cohorts (G1) spawned in March/April by (ii) overwintering cohorts (G). G overwintered with minimal to low growth, before undergoing rapid growth the following spring and completing the cycle by spawning the G1 generation and disappearing from the population by May/June. Our findings are discussed in the context of *L. helicina* response to climate change.

Keywords: life cycle, *Limacina helicina*, North Pacific, population dynamics, pteropod, seasonal growth.

Introduction

Thecosome pteropods comprise a group of calcifying holoplanktonic gastropod molluscs that are ubiquitous in pelagic marine ecosystems (Hunt *et al.*, 2008; Head and Pepin, 2010; Jennings *et al.*, 2010; Bednaršek *et al.*, 2012a, 2016; Beaugrand *et al.*, 2013). In the temperate and polar latitudes of both the northern and southern hemispheres, *Limacina helicina* tends to dominate the pteropod community. Regionally this species can comprise a significant component of total zooplankton biomass, represent an important grazer of primary producers, an important prey item for zooplanktivores, and contribute significantly to both organic and inorganic carbon flux (Lalli and Gilmer, 1989; Hunt *et al.*,

2008, 2014; Bernard and Froneman, 2009; Head and Pepin, 2010; Mackas and Galbraith, 2012; Doubleday and Hopcroft, 2015).

Limacina helicina appears to be highly responsive to changes in primary productivity (Maas *et al.*, 2011; Seibel *et al.*, 2012), with observations of massive population build up during phytoplankton blooms (Atkinson *et al.*, 1996), and population crashes when primary productivity is suppressed (Seibel and Dierssen, 2003). *Limacina helicina* would therefore be expected to be significantly impacted by climate-induced changes in primary productivity. This species is also temperature sensitive, as demonstrated by metabolic studies (Seibel *et al.*, 2007, 2012; Comeau *et al.*, 2010; Maas *et al.*, 2011) and long-term shifts in abundance and

Table 1. Summary of *Limacina helicina* life cycle parameters from the literature and this study. NA entries indicate non-available data.

Region	Spawn timing	Spawning behavior	Species	Gen/ year	Longevity (years)	Max. size (mm)	Peak density	T (°C)	Chl-a (mg·m ⁻³)	Bloom timing	Source
Arctic; Kongsfjorden	Spring and autumn	Discrete	LHH	1–2	1	13	Late summer	<5	~2	Spring	1, 6
Arctic; Canada Basin	Spring–summer–winter	Protracted; Summer peak	LHH	1	1.5–2	3.7	Spring–summer	<0	<0.5	Summer	2, 7
Antarctic; Scotia Sea	Summer	Discrete	LHA	1	≥3	≥10	Summer	<5	<10	Spring	4, 9
Antarctic Peninsula	NA	NA	LHA	1	1	<10	NA	<5	<10	Spring	5, 9
Station Papa, North Pacific	NA	NA	LHH	1	1	3.5	NA	~10	<0.5	Summer	3, 8
North-east Pacific; Rivers Inlet	Spring and summer	Continuous	LHH	2	≤1	5.5	Spring and summer	14.5	>30	Spring	This study

Also included are key environmental parameters (temperature, chlorophyll-a biomass and phytoplankton bloom timing) for the study regions. Gen, generations; LHH, *Limacina helicina helicina*; LHA, *Limacina helicina antarctica*.

References: 1. Gannefors *et al.* (2005); 2. Kobayashi (1974); 3. Fabry (1989); 4. Bednaršek *et al.* (2012b); 5. Hunt *et al.* (2008); 6. Hop *et al.* (2002); 7. Li *et al.* (2009); 8. Harrison (2002); 9. Holm-Hansen *et al.* (2004).

distribution in the north Atlantic and north Pacific related to changing temperature (Mackas and Galbraith, 2012; Beaugrand *et al.*, 2013). The latter may reflect a synergistic response to warming and decreased primary production (Zhai *et al.*, 2013).

Owing to their production of an aragonite shell, *L. helicina* are also particularly vulnerable to the effects of ocean acidification (Orr *et al.*, 2005; Fabry *et al.*, 2008). Aragonite is a metastable form of calcium carbonate that is susceptible to dissolution as ocean uptake of increasing anthropogenic CO₂ concentrations reduces pH and the saturation state of aragonite in seawater. The response of *L. helicina* to ocean acidification has been shown to be strongly coupled with temperature and metabolic rate (Comeau *et al.*, 2010; Lischka *et al.*, 2011; Lischka and Riebesell, 2012). Initial predictions were that the surface ocean would become undersaturated with respect to aragonite ($\Omega_{ar} < 1$) in future decades (Orr *et al.*, 2005; McNeil and Matear, 2008). However, with the growing body of data on ocean carbonate chemistry has come a growing number of observations of $\Omega_{ar} < 1$ conditions in the present day ocean associated with natural cycles, e.g. in association with sea ice melt in the Beaufort Sea (Yamamoto-Kawai *et al.*, 2009), upwelling in the California Current Ecosystem (Feely *et al.*, 2008), and glacial melt water in coastal fjords (Reisdorph and Mathis, 2014). Concomitant are observations of shell dissolution impacts on *L. helicina* associated with these aragonite undersaturated conditions (Bednaršek *et al.*, 2012, 2014).

The vulnerability of *L. helicina* to changing ocean conditions has potentially significant implications for ecosystem function, while also making this species a sentinel of environmental change (Bednaršek *et al.*, 2016). A key requirement for understanding an organism's response to change is knowledge of its life history. The temperate and polar regions where *L. helicina* is found are highly seasonal. The phenology of phytoplankton production and match/mismatch with *L. helicina*'s life cycle, as well as the quantity and quality of that production, are therefore expected to be important to the survival, growth, maturation, spawning success and recruitment of this species. The seasonal age and size structure, and depth

distribution of *L. helicina* may interact with productivity and temperature cycles, and the distribution of aragonite undersaturated waters, to affect differential survival over the course of its life cycle (Gannefors *et al.*, 2005; Hofmann and Todgham, 2010; Lischka *et al.*, 2011; Bednaršek *et al.*, 2014; Bednaršek and Ohman, 2015). Indications are that the smaller juvenile phases of this species may be particularly susceptible to starvation and ocean acidification (Gannefors *et al.*, 2005; Lischka *et al.*, 2011; Lischka and Riebesell, 2012; Thabet *et al.*, 2015; Manno *et al.*, 2016).

Although a number of studies have assessed the life cycle of *L. helicina*, considerable variability exists in the findings and/or their interpretation. We summarise these studies in Table 1. Key observations include a range of one to two generations per year; longevity of 1 to ≥3 years; maximum size range of 3.5–13 mm; peak densities from spring to late summer (Kobayashi, 1974; Fabry, 1990; Gannefors *et al.*, 2005; Hunt *et al.*, 2008; Bednaršek *et al.*, 2012b). This variability may be accounted for by a combination of regional differences in environmental conditions, and physiological (Rosenthal *et al.*, 2009; Seibel *et al.*, 2012) and genetic differences between taxonomic sub-units of this species, which has been shown to comprise two genetically distinct sub-species and up to five morphotypes (Lalli and Gilmer, 1989; Hunt *et al.*, 2010; Jennings *et al.*, 2010). However, a lack of high resolution annual time series of population structure may also have contributed to the variability in life cycle interpretation, and remains an important data gap in understanding *L. helicina*'s response to environmental change.

Rivers Inlet is a glacial fjord on the central coast of British Columbia (Canada) that is characterized by consistently high densities of *L. helicina*. Between 2008 and 2010 a comprehensive oceanographic program was conducted in the inlet, the Rivers Inlet Ecosystem Study (RIES). The RIES investigated the processes driving primary and secondary production in the inlet and included high temporal resolution sampling of the zooplankton community between spring and fall of each year, a daily time series between March and July of 2010, and 1 year of winter sampling in 2010/2011. Detailed analyses of the full zooplankton

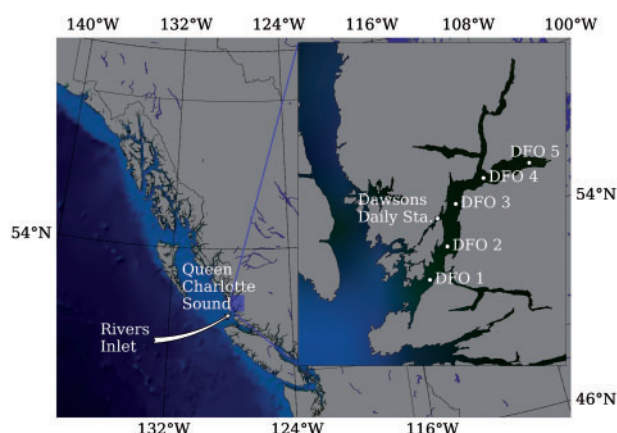


Figure 1. Map illustrating the location of Rivers Inlet on the coast of British Columbia, and location of oceanographic stations sampled during the Rivers Inlet Ecosystem Study (Inset), from 2008 to 2010. Daily sampling of zooplankton was maintained at Dawson's Landing in 2010.

community have been conducted elsewhere (Tommasi *et al.*, 2013a, b, 2014). Here we present an analysis data on the population structure of *L. helicina* from these time series, with the specific aim to determine the life cycle of this species with respect to its seasonal spawning activity, variability between years, and its growth, maximum sizes and longevity.

Methods

Data collection

Sampling was conducted across a set of five stations aboard the *MV Western Bounty*. For the purposes of this study our analysis focused on the station DFO2 which was approximately mid-way along the inlets length (330 m deep; Figure 1). Sampling at DFO2 was conducted every 2–3 weeks in 2008 (mid-March to mid-September) and 2009 (mid-March to mid-August), and monthly in 2010 (mid-March to mid-July). Between October 2010 and March 2011 net tows were collected at DFO2 on an ~3 weekly basis by the C'isliyaki research team, using the same methodology as the RIES. In 2010, an additional station was sampled daily off the docks at Dawson's Landing (30 m deep) (Figure 1).

Zooplankton sampling at DFO2 was conducted with a 0.50-m diameter bongo net (Aquatic Research Instruments) harnessed with 150 and 250 μ m mesh nets. Vertical hauls were conducted from 300 m to surface and the volume filtered for each net was determined with a General Oceanic's flowmeter. Only samples from the 150 μ m net were used in this study, with the exception of the 22 November 2010 sample for which 150 and 250 μ m mesh Bongo nets were combined because of small sample size. At the Dawson's Landing Daily Station zooplankton were sampled each day after dusk from 22 March to 7 July 2010 using a 0.30-m ring net fitted with 80 μ m mesh and hauled vertically from ~25 m to the surface (bottom depth 30 m). No flowmeter was used with this net and volume filtered was estimates from the depth of the haul assuming 100% filtration efficiency. Zooplankton samples from both DFO2 and the Daily Station were preserved with a 4% buffered seawater formaldehyde solution.

In addition to zooplankton, physical properties and phytoplankton biomass were measured in conjunction with each net

haul at DFO2 using a Seabrid SBE-25 CTD harnessed with a Wetlabs Wetstar fluorometer, deployed to a depth of 10 m from the bottom. At the Dawson's Landing Daily Station an RBR Concerto CTD with a Wetlabs Wetstar fluorometer was deployed on a daily basis to a depth of 2 m above the bottom at the same time as daily net sampling. Raw fluorescence values from both CTDs were converted to chlorophyll-a (chl-a) biomass ($\text{mg}\cdot\text{m}^{-3}$) using the factory calibrations. Here we present the temperature ($^{\circ}\text{C}$), salinity, and chl-a biomass data from the top 100 m at DFO2 to focus on the seasonal dynamics of each parameter in the euphotic zone. Vertical profiles of DFO2 survey data were plotted using ODV 4.7 (Schlitzer, 2017).

Sample processing

Limacina helicina shell diameter was measured to the nearest 0.1 μ m under a stereo microscope with an ocular ruler, from the tip of the shell aperture across the center of the shell. The 150- μ m bongo net samples from DFO2 were first scanned for large (>1 mm) *L. helicina* specimens. These were handpicked for enumeration and measurement from the entire sample to maximize retention of the larger and rarer population demographic. Each sample was subsequently split to a fraction comprising a minimum of 128 individuals from the remaining *L. helicina*. The 80 μ m ring net samples from the daily station were processed in their entirety to maximize the representativeness of the size structure data from these samples. A minimum of 128 *L. helicina* were measured and the remaining individuals counted for abundance estimates. The smaller size classes included late veliger stages ($\sim <0.3$ mm; Paranjape, 1968). Densities at both DFO2 and the Daily Station were expressed as individuals m^{-2} .

Data analysis

Two approaches were used to identify and track cohorts and estimate life cycle parameters:

Visual tracking of the means extracted from finite mixture distributions

Size frequency histograms were constructed for each sample collected at DFO2 and the Daily Station. At DFO2, measurements were binned into 0.2 mm intervals while *Limacina* sampled at the Daily Station were binned into 0.02 mm intervals. A smaller size-bin was selected for the Daily Station to assist detection of daily changes in population size structure. To maximize the ability to visually distinguish each cohort the data were not normalized.

Cohorts within each sample size distribution were identified using finite mixture distribution (FMD) modelling, implemented through the R package mixdist (R Core Team, 2013). This method applies a combination of expectation–maximization and a Newton-type algorithms to compute the best fit to the observed data from among a series of distribution types (normal, lognormal, exponential, and gamma). Mixdist allows the user to apply constraints on model parameters (e.g. number of cohorts, mean cohort size) to prevent overparameterization (Macdonald and Pitcher, 1979). In this study, the identification of cohorts was based on the appearance of distinct modal peaks in the size-frequency histograms. In cases when the size-frequency histograms lacked distinct modal peaks, the previous date of observation was used as a reference to estimate the most likely course of development through time. Subsequently, the mean

sizes attributed to different cohorts in any one sample were linked through time in a fashion thought to capture the growth trajectory of different, visually identified cohorts (Pauly, 1998).

The ability to track FMD identified cohorts varied between years, however, we were able to summarize the growth of two prominent cohorts annually. In 2008, up to three large cohorts (shell size range of 1–5 mm) were identified on each survey between 18 March and 22 April. We therefore did not attempt to track a single cohort through this size range. A major spawning event was observed on 9 May which allowed us to anchor a starting point for a spring generation (G1) (Figure 5). In 2009, we were able to track two main cohorts. The first of these, present on 28 February, was > 1.3 mm mean size (Cohort G), and the second was first observed on 3 May and had a mean size of 0.2 mm (Cohort G1; Figure 5). In 2010, a single large size cohort (G) was identified and tracked from 19 March to 17 May (Figure 5). Cohorts tracked are summarized in Table 3. Cohort-specific growth (GC) of *L. helicina* was estimated between each survey as the difference in the modal shell size of each cohort tracked between surveys, divided by the time elapsed between each survey, in days (d):

$$GC = \frac{M_j - M_i}{d}$$

where M is the modal shell size (mm) of each cohort tracked and i and j are the previous and current survey, respectively.

Using the higher resolution daily data, 24 cohorts were identified from late March to early July 2010, and each was tracked for variable lengths of time. Observations of strong overlap in the modal shell-size between numerous cohorts for various lengths of time (up to 34 d; Supplementary Material, Figures S1–S8; Table S1) complicated our calculations of daily growth rates. Consequently, an average modal shell-size of cohorts was calculated for the days of overlap and used to estimate the mean population level growth rate between days. Owing to the low frequency of occurrence of individuals > 1 mm only individuals < 0.5 mm were considered in the analysis of daily data. We individually tested the relationship between temperature and chlorophyll-*a* and daily growth rates using simple linear regression, and combined affects with a generalized additive model (GAM) using the R package mgcv. Both same day and 1 d lagged analyses were performed.

Longevity was estimated as the difference in days between the date of detection and the date of estimated die-off of a cohort (disappearance from the population).

Estimating the parameters of seasonally oscillating von Bertalanffy growth functions

The von Bertalanffy growth function (VBGF) is one of the standard models of fishery science; for length, the VBGF has the form (von Bertalanffy, 1938):

$$L_t = L_{\infty} \cdot (1 - e^{-K \cdot (t - t_0)})$$

where L_t is the length at age t , L_{∞} is the asymptotic length (roughly corresponding to the maximum length in the population in question), K is a parameter of dimension time^{-1} , expressing how fast L_{∞} is approached, and t_0 is the (usually negative) age at size = 0 (and not discussed further here).

However, while the standard VBGF is appropriate for relatively long-lived fish or invertebrates, whose growing phase occurs over several years, it cannot be used to describe the growth of short-lived animals, in which most of the growth occurs within a year. In such cases, seasonal growth oscillations must be considered explicitly. This is done here through a variant of the VBGF (Somers, 1998; Pauly, 1998) of the form

$$L_t = L_{\infty} \cdot \{1 - \exp[-K(t - t_0) + S(t) - S(t_0)]\}$$

where L_{∞} , K , and t_0 are defined as in the standard VBGF (see above), and where

$$S(t) = (CK/2\pi) \cdot \sin \pi(t - t_s) \text{ and } S(t_0) = (CK/2\pi) \cdot \sin \pi(t_0 - t_s).$$

This equation involves two parameters more than the standard VBGF: C and t_s . The former of these expresses the amplitude of the growth oscillations. When $C = 0$, the seasonally oscillating VBGF reverts to the standard VBGF. When $C = 0.5$, the seasonal growth oscillations are such that growth rate increases, e.g. by 50% at the peak of the ‘growth season’, i.e. in ‘summer’, and, briefly, declines by 50% in ‘winter’. When $C = 1$, growth increases by 100%, i.e. doubles during ‘summer’, and becomes zero in the depth of ‘winter’.

The second new parameter, t_s , expresses the time between $t = 0$ and the start of a sinusoid growth oscillation. For visualization, it is useful to define $t_s + 0.5 = \text{WP}$ (Winter Point), which expresses, as a fraction of the year, the period when growth is slowest.

The fitting of growth curves to length-frequency data by ELEFAN is performed through a non-parametric optimization procedure described in detail in Pauly (2013).

Results

Environmental conditions

Water column profiles showed a seasonal warming of a low salinity surface layer in the upper 5 m beginning in April/May (Figure 2). This low salinity surface layer represented discharge from the Wannock River which drains the glacial dominated Owikeno Watershed. Wannock discharge is at its minimum from January to March and maximum from May to July, during the freshet (Hodal, 2011; Pickard, 1961). The freshet is the sudden increase in river flow following the spring melting of the annual snowpack. Maximum temperature attained in this surface layer was ~14.5 °C. Below the low salinity surface layer, seasonal warming to > 8 °C was observed through the upper > 50 m. This water column warming was weakest in 2009, and was more uniformly warm in 2010 compared with 2008 and 2009. Spring conditions differed between years and were coolest in 2009 (< 7 °C) and warmest in 2010 (~7.5 °C). Water temperatures averaged over the upper 30 m of the water column increased from spring to summer for all years (Figure 3), and were ~1 °C higher in 2010 compared with 2009. Temperatures in 2008 were intermediate between 2010 and 2009 until July when 2009 temperatures exceeded 2008. Temperature data at the daily station (Dawsons) corresponded well with the data at DFO2, though with greater variability associated with freshwater input (low salinity anomalies).

The dominant feature of the salinity profiles was the fresh surface layer (upper 5 m) associated with the Wannock River

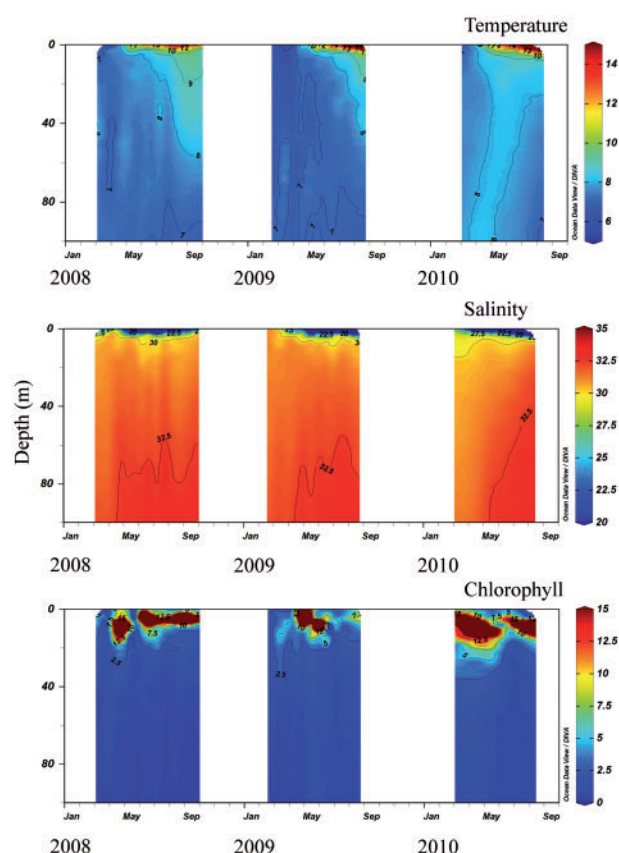


Figure 2. Vertical profiles of temperature ($^{\circ}\text{C}$), salinity (psu), and chlorophyll-a biomass ($\text{mg}\cdot\text{m}^{-3}$) through the upper 100 m of the water column at DFO2 from 2008 to 2010.

discharge (Figure 2). Surface salinity values of 7.48, 8.04, and 11.87 on 10 July 2008, 17 June 2009, and 21 June 2010, respectively, signaled the peak of the freshet in each year. Below the surface freshwater layer, salinity was lower in March, April, and May of 2010 than in 2008 and 2009 and this was reflected in the 30 m average salinity values (Figure 3). From June, however, the mean values converged for all 3 years. Salinity at the daily station tended to be slightly lower than at DFO2 in 2010, influenced by freshwater runoff at this site.

Phytoplankton biomass was concentrated in the upper 20 m of the water column and reached maximum values of $>30 \text{ mg}\cdot\text{m}^{-3}$ during the spring and summer blooms (Figures 2 and 3). The spring bloom was initiated on ~ 7 April in 2008 and persisted until ~ 11 May when it subsided. A second, summer bloom developed on ~ 26 May and persisted until the last survey on 26 September. The spring bloom in 2009 was the latest, occurring on ~ 3 May. This bloom persisted until ~ 17 June at the 5–10 m depth range after which the phytoplankton biomass declined and remained at a low level through the remainder of the summer. In 2010, the spring bloom was already underway at the time of the first survey on 19 March. High phytoplankton biomass ($\geq 16 \text{ mg}\cdot\text{m}^{-3}$) was initially observed in the 3–15 m depth range but shifted deeper in the water column through to 18 May, indicating nutrient depletion in the surface waters. The spring bloom terminated on ~ 18 June and a second, summer bloom was

initiated at 5 m depth on 21 June, which persisted until the date of the last survey on 20 July. Depth integrated (30 m) phytoplankton biomass reflected the seasonal pattern described above (Figure 3). Integrated phytoplankton biomass at the daily station in 2010 was lower than at DFO2 (Figure 3). Two peaks in biomass were observed, one in mid-April and the other in late May/early June.

Limacina helicina seasonal abundance and population size structure

In 2008, the 18 March sample was notable for low densities of *L. helicina*, a complete absence of juveniles, and a mean shell size of 1.55 mm (Table 2; Figure 4) for three identified population components of generation G (Figure 5). The mean shell size of G rapidly increased through to a maximum of 5.5 mm on 9 May. The 25 May was the last time that specimens >4 mm were recorded in the population in 2008. On 9 May, the mean shell size decreased to 0.87 mm, corresponding with a peak in abundance of $>150\,000 \text{ ind}\cdot\text{m}^{-2}$, indicating a recruitment event. After 9 May juveniles were constantly present in the population until 4 August. Densities decreased to $<50\,000 \text{ ind}\cdot\text{m}^{-2}$ by July and remained at that level until late September. Despite the constant presence of juveniles, the mean shell size increased from 0.9 mm on 9 May to 1.1 mm on 4 August, with a maximum size of 3.78 mm. The FMD analysis tracked the growth of the 9 May population component (G1) from a modal peak of 0.20 mm on that date to 2.2 mm (max = 3.78 mm) on 4 August (Table 3), and it is likely that this cohort contributed most to the increase in mean population shell size over that period. By the final sampling event on 22 September, these large late summer specimens had disappeared from the population, and mean shell size had decreased to 0.5 mm (maximum = 2.65 mm).

In 2009, *L. helicina* densities were low on 28 February and remained at $<10\,000 \text{ ind}\cdot\text{m}^{-2}$ until 2 June after which they increased to a peak of $>30\,000 \text{ ind}\cdot\text{m}^{-2}$ on 13 August (Figure 4). Two population components were evident on 28 February, with modal shell sizes of 1.3 mm (G generation) and 0.2 mm (G1 generation) (Table 3; Figure 5). By 20 May G had mostly disappeared, though some of this component persisted until 17 July when they had a modal shell size of 4.4 mm (Figure 5; Table 3). As in 2008, juveniles were present throughout the summer (Figures 4 and 5). A reduction in population mean size was observed on 15 April/3 May (<0.5 mm) and again on 13 August, the latter coinciding with the highest densities for 2009 indicating a substantial recruitment event (Figure 4). The maximum size on 13 August was 3.4 mm, similar to the mean size of 3.3 mm estimated to have been attained by this date for *L. helicina* hatched on 3 May (Component G1, Table 3).

In 2010, *L. helicina* abundance peaked at $>40\,000 \text{ ind}\cdot\text{m}^{-2}$ on 17 May and 21 June at the Daily Station and DFO2 (Figures 4 and 6). These peaks corresponded with a decline in mean size indicating that they were associated with recruitment events (Figure 6). As in 2009, two population components were evident in spring, with modal sizes of 2.7 mm (G generation) and 0.2 mm (G1 generation) (Figure 5; Table 3). G grew to a maximum size of 5.3 mm on 17 May (mean = 4.2 mm). No individuals larger than 4.1 mm were observed on the June and July surveys. We did not consider the Daily Station data in interpreting the G generation. Large *L. helicina* (>3 mm) were undersampled at the Daily

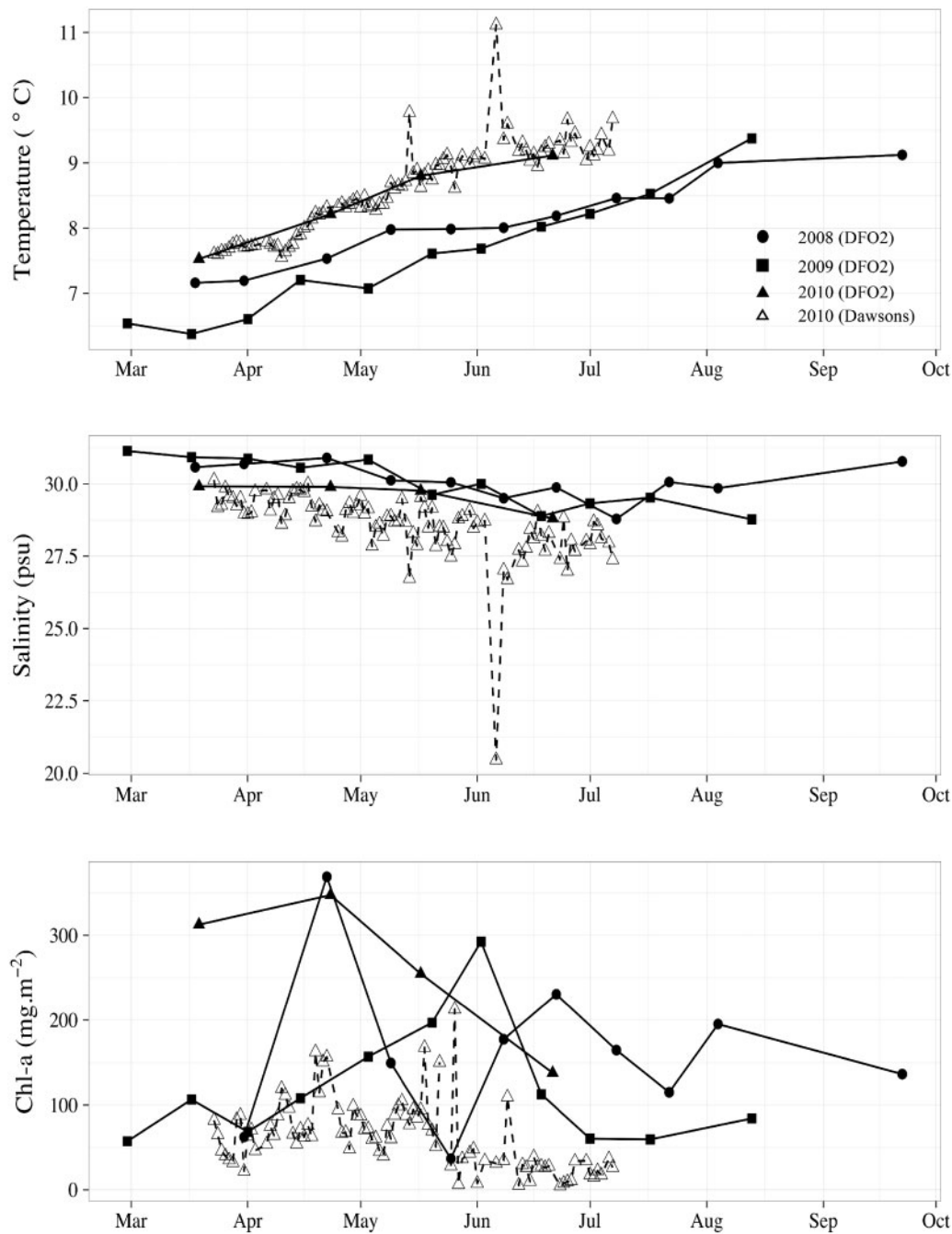


Figure 3. Seasonal variation in temperature (°C), salinity (psu), and chlorophyll-a biomass (mg·m⁻²) averaged over the upper 30 m of the water column at DFO2 in 2008, 2009, and 2010, and the daily station at Dawson's Landing in 2010.

Station, most likely because of this site being shallow (<30 m), and the larger individuals being deeper in the water column (Kobayashi, 1974). As in 2008 and 2009, juveniles were present on all summer surveys (Figures 4 and 5).

The fall/winter samples collected in 2010–2011 (October 2010 to March 2011) had abundance levels <5000 ind·m⁻², similar to the pre-spring peak levels observed in 2008, 2009, and 2010 (Figure 4). The 22 November samples were the first in the time series to show an absence of juvenile *L. helicina*. Mean size was ~0.7 mm and maximum size ~2.54 mm (Table 2). These data,

and the data from September 2008, indicated that the large (>3 mm) late summer G1 specimens had disappeared from the population by autumn. Slight winter growth was observed from a low mean size of 0.63 mm on 8 November to 0.84 mm in February (Table 2).

Growth rates and longevity

In 2008, Cohort G1 exhibited the lowest estimated growth rates on 25 May (0.006 mm·d⁻¹), increasing with each survey to a maximum of 0.06 mm·d⁻¹ on 8 July, before decreasing to

Table 2. Dates of net samples collected at DFO2 in Rivers Inlet in 2008, 2009, 2010, and 2011 from which *Limacina helicina* abundance and size frequency were analysed.

Year	Day and month	Mean size (mm)	Minimum size (mm)	Maximum size (mm)
2008	18 March	1.55	0.17	3.00
2008	31 March	1.75	0.17	3.00
2008	22 April	2.86	0.21	4.11
2008	09 May	0.87	0.13	5.50
2008	25 May	1.39	0.18	4.83
2008	08 June	0.51	0.12	3.45
2008	22 June	0.80	0.16	3.78
2008	08 July	0.98	0.16	3.35
2008	04 August	1.10	0.14	3.78
2008	22 September	0.51	0.18	2.65
2009	28 February	0.68	0.18	2.64
2009	17 March	0.99	0.22	2.43
2009	01 April	0.89	0.18	3.58
2009	15 April	0.49	0.12	3.63
2009	03 May	0.41	0.18	3.91
2009	20 May	0.57	0.13	4.42
2009	02 June	0.75	0.18	4.42
2009	18 June	0.64	0.17	2.82
2009	01 July	0.72	0.13	4.65
2009	17 July	0.66	0.13	4.42
2009	13 August	0.55	0.17	3.39
2010	19 March	0.62	0.21	2.74
2010	23 April	0.37	0.15	3.61
2010	17 May	1.04	0.16	5.30
2010	21 June	1.65	0.16	4.06
2010	20 July	1.11	0.16	3.56
2010	25 October	0.72	0.20	2.03
2010	08 November	0.63	0.29	2.43
2010	22 November	0.69	0.19	2.54
2011	18 January	0.73	0.23	1.84
2011	08 February	0.84	0.51	2.10
2011	19 March	0.50	0.21	0.56

The mean minimum, and maximum size (mm) of *L. helicina* is indicated. All samples were collected with 150 μm Bongo nets, with the exception of the 22 November 2010 sample for which 150 and 250 μm mesh Bongo nets were combined.

0.01 $\text{mm}\cdot\text{d}^{-1}$ by early August (Table 3). In 2009, the G cohort exhibited comparatively rapid growth rates until 1 April, reaching 0.06 $\text{mm}\cdot\text{d}^{-1}$ before declining to negligible growth by 17 July. The G1 cohort in 2009 initially demonstrated slow growth (0.01 $\text{mm}\cdot\text{d}^{-1}$), maintained relatively high growth through June and July (0.04–0.6 $\text{mm}\cdot\text{d}^{-1}$), before decreasing to 0.01 $\text{mm}\cdot\text{d}^{-1}$ in August. In 2010 the G cohort demonstrated relatively slow growth in late April (0.01 $\text{mm}\cdot\text{d}^{-1}$) before increasing to 0.04 $\text{mm}\cdot\text{d}^{-1}$ in mid-May. Estimated *L. helicina* growth rates from the Daily Station in 2010 were highly variable but had a mean of 0.03 $\text{mm}\cdot\text{d}^{-1}$ (Figure 6; minimum = 0.0005 $\text{mm}\cdot\text{d}^{-1}$; maximum = 0.08 $\text{mm}\cdot\text{d}^{-1}$). Owing to the continuous spawning through the spring and summer it is likely that this value was an underestimate, although in the range of values estimated from DFO2 and very similar to the mean growth rate of 0.029 $\text{mm}\cdot\text{d}^{-1}$ from that station (Table 3). Linear regression analysis found that temperature and chl-a explained little of the variance in daily growth rates, the relationship being highly non-significant for both same day and lagged data ($p > 0.15$; $R^2 < 0.05$). The best fit occurred when growth rates were lagged by 1 d (Supplementary Material, Figures S9 and S10). Similarly, the GAM model combining temperature and chl-a explained <2.5% of the variation in daily growth rates (Supplementary Material, Figure S11).

Application of ELEFAN and of the seasonally oscillating version of the VBGF

Although there is, throughout the year, a continuous recruitment of *L. helicina*, the length-frequency data analysed by ELEFAN allowed the identification of two major cohorts per year, an overwintering cohort, corresponding to cohort G, and a summer cohort, corresponding to G1 (Figure 7). The asymptotic size of the overwintering cohorts were estimated as ranging from 5.03 to 5.84 mm, while K were estimated as 4.17–3.80 year^{-1} (see Figure 7, right panels). The asymptotic lengths of the summer cohorts were smaller (4.18–4.98 mm), with the K estimates correspondingly higher (5.14–4.94 year^{-1} (see Figure 7, right panels).

Note, however, that the shape of the best fitting curves that were identified by ELEFAN (Figure 7), especially for the overwintering cohorts, was primarily shaped by strong seasonal oscillations, described by the additional parameters $C=1$, and $WP=0.9$ for the overwintering cohorts and $C=0.4$, $WP=0.1$ for summer cohort, respectively. Our interpretation of Figure 7 (left panels) is that it depicts overwintering cohorts (G) consisting of individuals which grew very little from November to January, but grew rapidly from February on, to reach a maximum size at May/June, suggesting a longevity of about 10 months. In contrast,

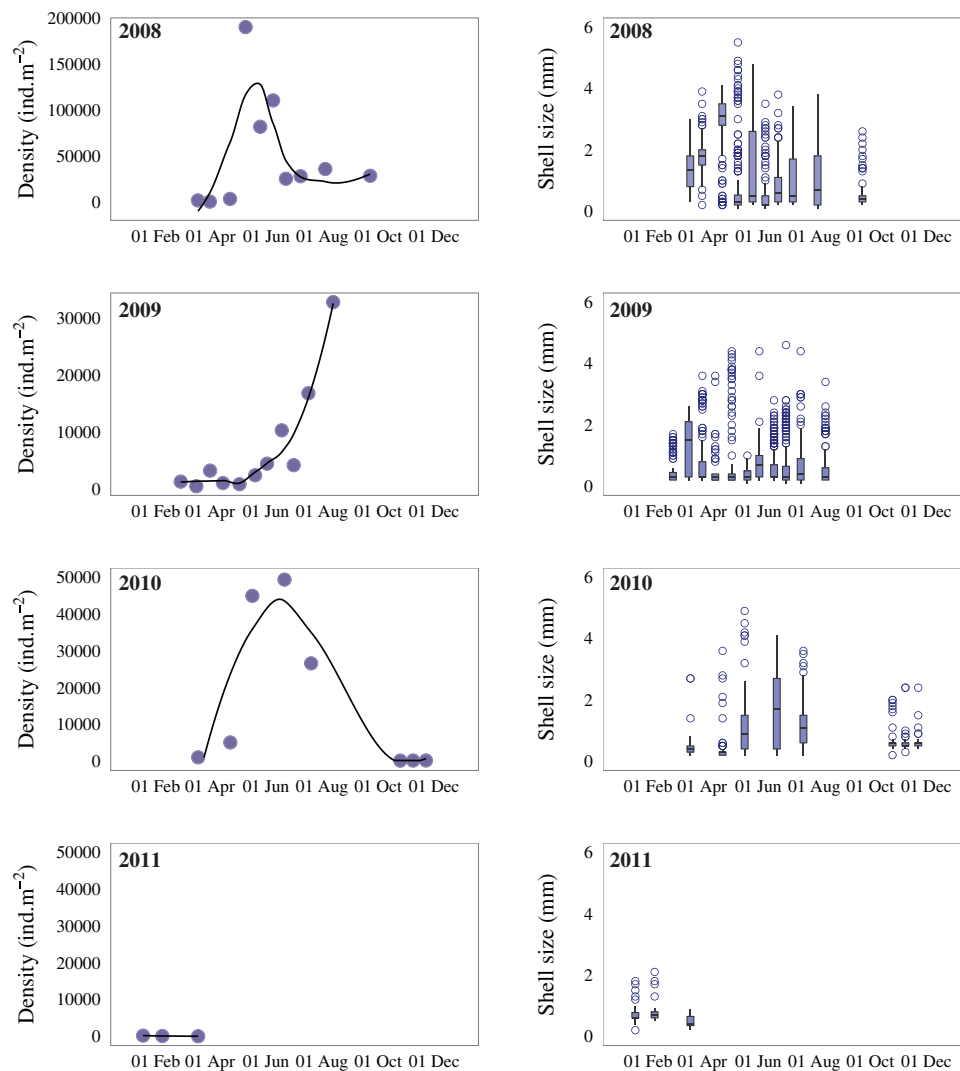


Figure 4. Seasonal variation of *Limacina helicina* (left column) abundance (ind.m⁻²), with a loess smoother (solid black line) fitted through the data from each year; and (right column) size structure (mm) displayed as box plots for DFO2 in 2008, 2009, 2010, and 2011. The black horizontal line of each box represents the median shell size. The upper and lower edges of the box denote the approximate first and third quartiles, respectively. The vertical error bars extend to the lowest and highest data value inside a range of 1.5 times the inter-quartile range, respectively. Points indicate extreme values. Note the differences in Y-axis limits between each year for the abundance data.

the summer cohorts (G1; left panels in Figure 7) had lower asymptotic length and a higher K , and appeared to complete their life cycle in an even shorter time.

Discussion

The three years of high temporal resolution abundance and size frequency data for *L. helicina* collected during this study enabled a detailed analysis of this species' life history parameters. Differences were observed between years, which we discuss in detail below. We begin by providing a life cycle overview, emergent from these data.

The life cycle of *Limacina helicina*

Based on the combined abundance and size frequency data we can summarize the life cycle of *L. helicina* in Rivers Inlet as follows (Figure 8). A spring generation (G1) is spawned in March/

April by an overwintering generation (G). Spring spawning enables the G1 generation to take advantage of the spring bloom and summer production, allowing rapid growth to maturity by July/August when they spawn a second generation, G. Growth rate estimates support this—assuming a spring spawning date of 1 May, a spawn size of 0.15 mm, and a mean growth rate of 0.03 mm.d⁻¹, *L. helicina* are able to reach a shell size of 3 mm by 5 August. The size structure data for the winter months indicates that the G1 generation disappears from the population after spawning. The G generation overwinter with minimal to low growth, before undergoing rapid growth the following spring and completing the cycle by spawning the G1 generation, then disappearing from the population by May/June. Accordingly we estimate that the G1 generation lives for ~6 months and grows to a maximum shell diameter of 3.5 mm, and the G generation lives for up to ~11 months and grows to a maximum shell size of

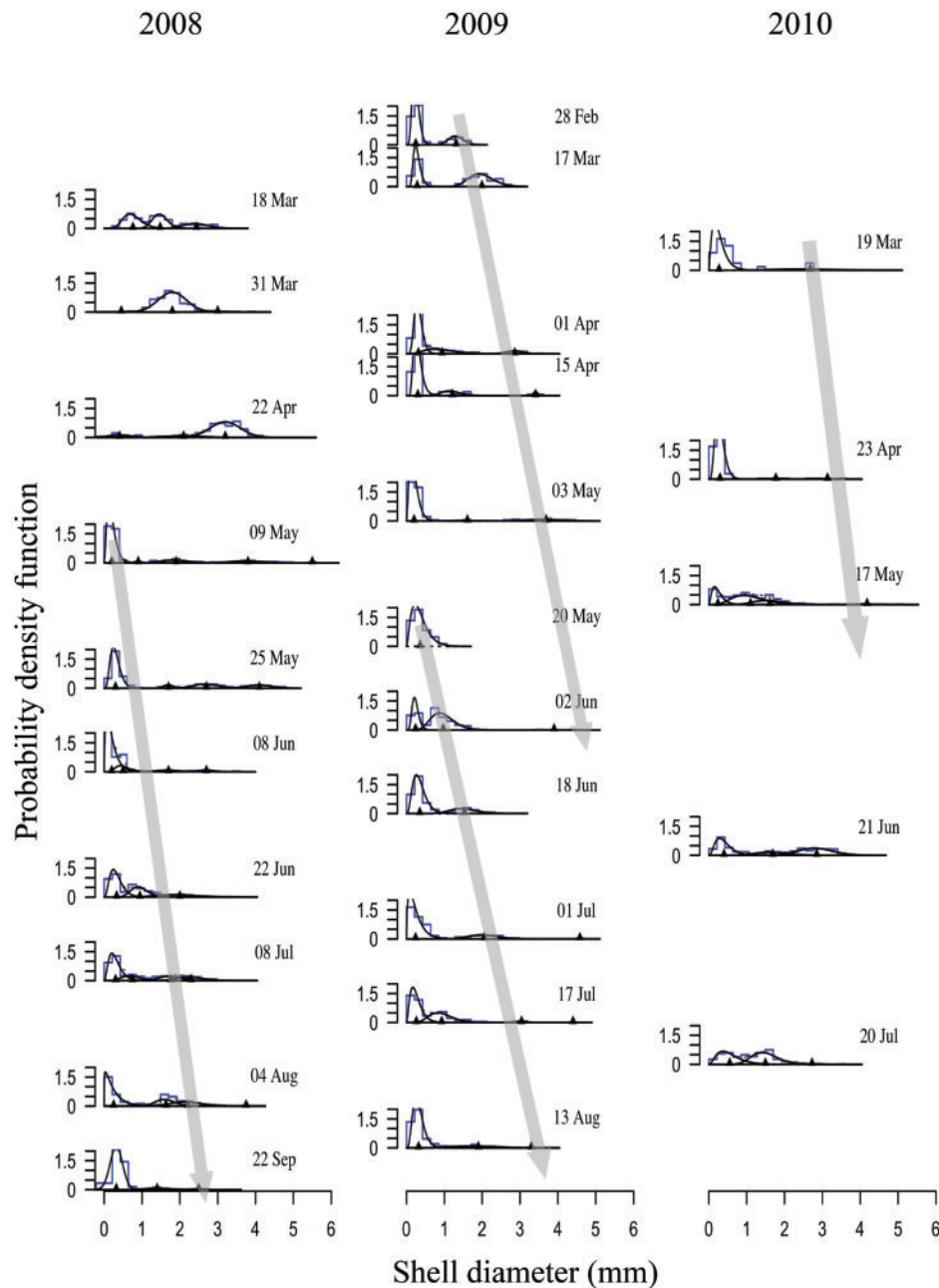


Figure 5. Finite mixture distributions fitted to the size-frequency data for *Limacina helicina* from surveys conducted in 2008, 2009, and 2010 at station DFO2 in Rivers Inlet. Shell diameter (mm) is represented on the x-axis and probability density on the y-axis. Note that the y-axis range differs between figures. The figures include size frequency histograms; the overall population distribution (thin black line); and the distribution of each population component that when combined forms the overall distribution, with triangles indicating the modal shell size (mm) of each component. Survey dates are indicated for each subplot and correspond to the survey dates in Table 2 and 3. Grey arrows indicate the approximate direction of growth of the overwintering and spring generations. The actual modal sizes used for tracking each generation, and associated growth rate estimates, are indicated in Table 3.

5.5 mm. The observation of two seasonal biomass peaks for *L. helicina* off the west coast of Vancouver Island (British Columbia), in spring and autumn, indicates that the general life cycle presented above is applicable to the broader region (Mackas and Galbraith, 2012).

A feature of the *L. helicina* population size structure data was that apart from spring 2008, the only time that juveniles were not

present in the population was during the winter of 2010/2011. Therefore, in addition to the two main spawning periods, there was ongoing low level spawning through the spring and summer months. The only other high resolution time series for *L. helicina*, from the central Arctic ocean, also observed ongoing spawning from May to the onset of winter (Kobayashi, 1974). That study did observe limited spawning in the winter months, suggesting

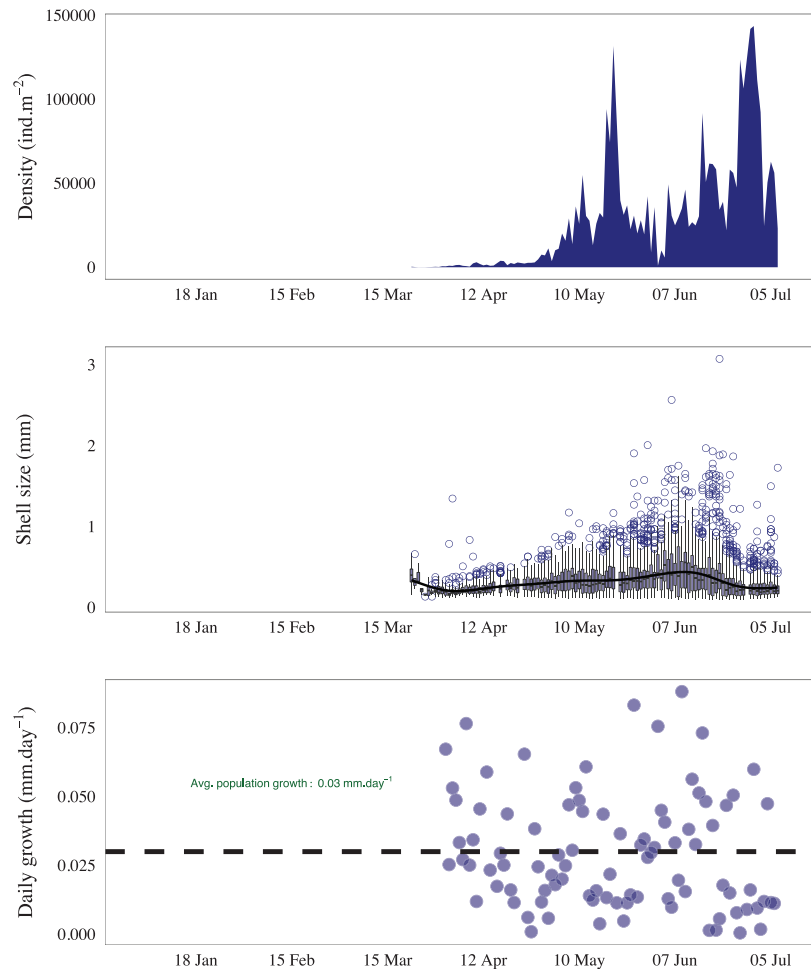


Figure 6. Daily variation of *Limacina helicina* (upper panel) density (ind.m^{-2}); (middle panel) size structure (mm), presented as box plots with a loess smoother (solid black line) fitted to highlight the seasonal trend; and (lower panel) average daily growth rate (mm d^{-1}) of each cohort identified and tracked for the period 22 March to 7 July 2010 at the Daily Station, with the black dashed line indicating the average cohort growth rate for the entire time series (0.03 mm d^{-1}). In the box plots the black horizontal line of each box represents the median shell size. The upper and lower edges of the box denote the approximate first and third quartiles, respectively. The vertical error bars extend to the lowest and highest data value inside a range of 1.5 times the inter-quartile range, respectively. Points indicate extreme values. Note the differences in Y-axis limits between each year for the abundance data.

that this may be a possibility in the North Pacific. The presence of juveniles in late February and March indicates that spawning may occur at least in the late winter in the study area.

Interannual life cycle variability of *Limacina helicina*

The three years of this study differed with respect to environmental conditions. In 2008, temperature and salinity were mid-range, while 2010 was the warmest and freshest. Spring temperatures in 2010 were 1°C warmer than 2009. Correspondingly, 2010 was the year for which ELEFAN estimated the lowest asymptotic length (Figure 7), which is consistent with the inverse relationship between temperature and the asymptotic size of fish and aquatic invertebrates (Pauly, 1998). The years 2008 and 2010 had high phytoplankton biomass from April to at least July. In comparison, the spring bloom was one month later in 2009, and that year had a relatively short lived high phytoplankton biomass period (May to mid-June). Although *L. helicina* spawning did occur in spring 2009, evident in the presence of

juveniles in late February and March, the low abundance of the G generation indicated either that spawning was reduced or that survival of juveniles was low. We suggest that this reflected a negative response of *L. helicina* to the delayed late spring phytoplankton bloom in 2009, as has been demonstrated for *L. helicina antarctica* in the Ross Sea (Seibel and Dierssen, 2003; Maas *et al.*, 2011).

Life cycle comparison with previous studies

The life cycle model that we present here for the *L. helicina* shows both similarities and differences to previous life cycle interpretations for this species (Table 1). One potential factor in the observed variation is environmental conditions, particularly primary productivity (Seibel and Dierssen, 2003; Maas *et al.*, 2011) and temperature (Seibel *et al.*, 2007, 2012; Lischka *et al.*, 2011). Spring and autumn spawning events were reported for *L. helicina* in Kongsfjorden (Spitsbergen, Arctic; Gannefors *et al.*, 2005), and longevity was proposed as 1 year. Environmentally, Kongsfjorden is significantly

Table 3. Growth rates (mm·day⁻¹) of cohorts identified from fortnightly / monthly data collected at DFO2 between 2008 and 2010.

Year	Day and month	Cohort	Modal shell size (mm)	Growth (mm·d ⁻¹)
2008	09 May	G ₁	0.20	NA
2008	25 May	G ₁	0.30	0.006
2008	08 June	G ₁	0.50	0.014
2008	22 June	G ₁	0.95	0.031
2008	08 July	G ₁	1.70	0.047
2008	22 July	G ₁	NA	NA
2008	04 August	G ₁	2.20	0.019
2008	22 September	G ₁	2.50	0.006
2009	28 February	G	1.31	NA
2009	17 March	G	1.99	0.040
2009	01 April	G	2.86	0.058
2009	15 April	G	3.41	0.039
2009	03 May	G	3.69	0.015
2009	20 May	G	NA	NA
2009	02 June	G	3.90	0.007
2009	18 June	G	NA	NA
2009	01 July	G	4.58	0.023
2009	17 July	G	4.40	NA
2009	03 May	G ₁	0.20	NA
2009	20 May	G ₁	0.36	0.009
2009	02 June	G ₁	0.97	0.047
2009	18 June	G ₁	1.53	0.035
2009	01 July	G ₁	2.05	0.040
2009	17 July	G ₁	3.04	0.062
2009	13 August	G ₁	3.30	0.009
2010	19 March	G	2.68	NA
2010	23 April	G	3.13	0.013
2010	17 May	G	4.18	0.044
2010	21 June	G	NA	NA
2010	20 July	G	NA	NA

Entries of NA indicate either a first occurrence of an identified cohort, or that the cohort was not detected in a size-frequency histogram in the time series.

cooler than Rivers Inlet, however, that fjord is also characterized by a spring phytoplankton bloom and relatively high phytoplankton biomass through summer and autumn (Hop *et al.*, 2002). Similar to Gannefors *et al.* (2005), Fabry (1989) estimated a 1 year life cycle for *L. helicina* in the North Pacific. In the high Arctic Ocean, Kobayashi (1974) observed protracted spawning between later winter and late autumn with evidence for a mid-summer peak (May–July), and suggested a longevity of 1.5–2 years. The high Arctic Ocean is oligotrophic and experiences a low intensity summer bloom, which together with the cold temperatures may account for the protracted lifespan and smaller size attained by *L. helicina* in this region. In both Kongsfjorden and Rivers Inlet, *L. helicina* attained at least double the size of specimens in the high Arctic (Table 1). In the Southern Ocean, two contrasting life cycles are presented for *L. helicina*, sub-species *antarctica*, with interpretations of a 1 year life cycle (Hunt *et al.*, 2008) and 3 year life cycle (Bednaršek *et al.*, 2012b).

A potentially key factor in observed life cycle variability may be genetic differences between taxonomic sub-units of this species. *Limacina helicina* has been shown to comprise two genetically distinct sub-species and up to five morphotypes (Lalli and Gilmer, 1989; van der Spoel *et al.*, 1999; Hunt *et al.*, 2010; Jennings *et al.*, 2010). Currently, northern and southern hemisphere *L. helicina* are listed as the sub-species *L. helicina helicina* (morphotypes—*acuta*,

helicina, and *pacifica*) and *L. helicina antarctica* (morphotypes—*antarctica* and *rangi*) respectively. These forms typically have different geographical ranges and may be representative of different life cycle adaptations.

Finally, we note the similarities between the life cycle for *L. helicina* identified in this study and that of the congeneric species *L. retroversa*. The latter species has been reported to have two generations per year, with spring and autumn spawning events, in both the Southern Argentine Sea (Dadon and de Cidre, 1992) and the west Atlantic (Lalli and Gilmer, 1989; Thabet *et al.*, 2015). The detailed size structure data presented by Dadon and de Cidre (1992) showed that an overwintering generation spawns a new generation in the spring when at a minimum size of 1.99 mm and maximum of ~3.25 mm. Soon after spawning the overwintering generation dies. The spring generation goes on to produce a second generation in the autumn that overwinters to the following spring. The spring generation undergoes rapid summer development but reaches a smaller size than the overwintering generation (minimum size = 1.25 mm), as observed for *L. helicina* in Rivers Inlet. Long-term observations from the Mediterranean Sea for pteropods broadly grouped as Limacinidae support a two generation per year life cycle for this family (Howes *et al.*, 2015).

Implications of *L. helicina* life cycle in a changing North Pacific

As highlighted in the introduction, the smaller juvenile phases of this species may be particularly vulnerable to starvation and ocean acidification (Gannefors *et al.*, 2005; Lischka *et al.*, 2011; Lischka and Riebesell, 2012). In this context, the life cycle that we identify for *L. helicina* in Rivers Inlet points to two key times of vulnerability for this species annually, the spring and autumn. Variability and long-term change in oceanographic conditions at these times may be critical to the recruitment success and persistence of *L. helicina*. Long-term changes in spring bloom timing in this region (Wolfe *et al.*, 2015) may therefore be an important source of variation in *L. helicina* abundance through match/mismatch impacts on spring recruitment. Similarly, changes in primary productivity through the summer months associated with long-term trends in freshwater discharge (Hodal, 2011) would be expected to impact recruitment to the overwintering population of *L. helicina*, with implications for spawning stock biomass in spring of the following year. Although our preliminary analyses found no correlation between daily growth rates and temperature and/or phytoplankton biomass, this is an important area of research for understanding the response of *L. helicina* to environmental conditions. It is possible that this response may lag environmental conditions by more than the 1 d analysed in this study.

As with the timing of the phytoplankton bloom, the timing of occurrence of aragonite undersaturated conditions in the upper water column may determine the impact of such conditions on *L. helicina*. Aragonite undersaturated surface ocean conditions have been reported from the present day north-east Pacific, associated with natural summer/fall glacial melt water in British Columbia and Alaska (Reisdorph and Mathis, 2014; Moore-Maley *et al.*, 2016), and upwelling in California (Feely *et al.*, 2008). Shifts in the timing of these aragonite undersaturation events relative to the life cycle of *L. helicina* may be critical to this species response to ocean acidification.

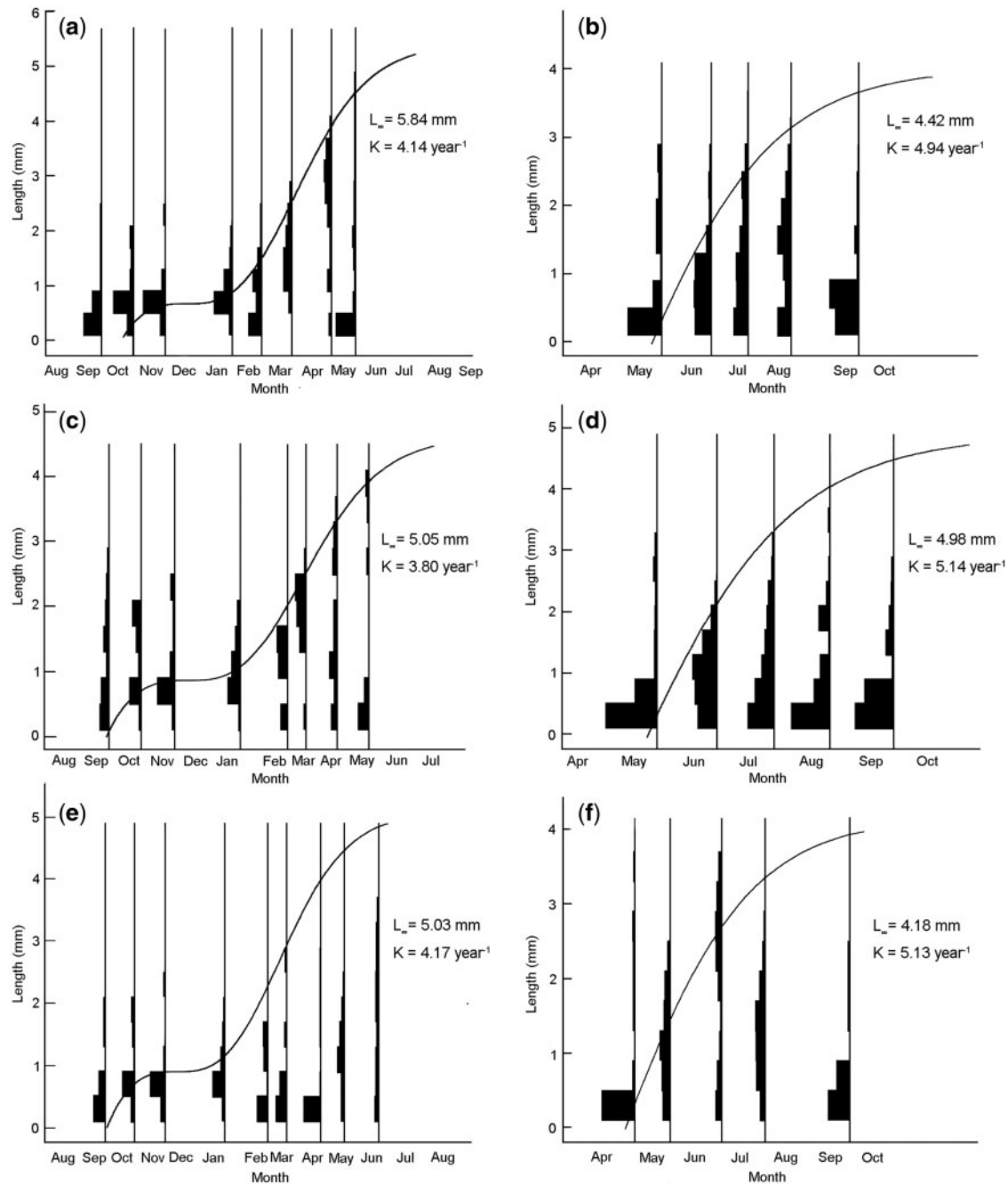


Figure 7. Seasonally oscillating versions of the von Bertalanffy Growth Function fitted by ELEFAN to length–frequency data of *Limacina helicina*. Left panels: overwintering cohort G (with $C = 1$ and $WP = 0.9$). Right panels: summer cohort (with $C = 0.4$ and $WP = 0.1$). (a, b) Overwintering cohort (September 2007–May 2008) and summer cohort (May–September 2008); (c, d) Overwintering cohort (September 2008–May 2009) and summer cohort (May–September 2009); (e, f) Overwintering cohort (September 2009–April 2010) and summer cohort (April–September 2010).

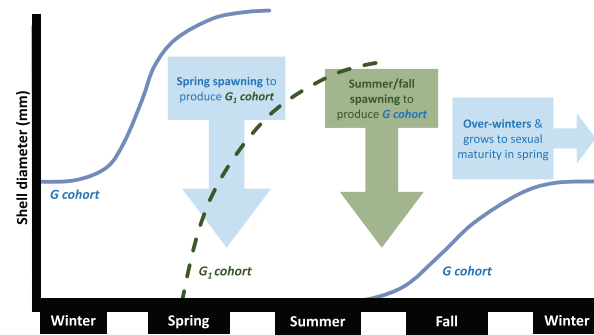


Figure 8. Conceptual life cycle model for *Limacina helicina* in the North Pacific. Seasons are indicated on the x-axis and shell size (mm) on the y-axis. Two generations are depicted: G (solid line) with a lifespan of ~ 11 months and a maximum size of 5.5 mm ($L_{\infty} = 5.5$); and G_1 (dashed line) with a lifespan of ~ 6 months and a maximum size of < 4 mm ($L_{\infty} < 5$ mm). Periods of peak spawning (spring and late summer / autumn) are depicted by the large downward pointing arrows.

Supplementary data

Supplementary material is available at the ICESJMS online version of the manuscript.

Acknowledgements

The Rivers Inlet Ecosystem Study (RIES) was funded by the Tula Foundation. We thank the University of British Columbia, Simon Fraser University, and Wuikinuxv First Nation members of the RIES research team for making this sample collection program possible, and Wayne Jacob and the C'isliyaki research team for collecting the winter samples of 2010/11. Cui Liang acknowledges financial support from the China Scholarship Council. Daniel Pauly acknowledges support from the Paul G. Allen Family Foundation via the Sea Around Us.

References

- Atkinson, A., Shreeve, R. S., Pakhomov, E. A., Priddle, J., Blight, S. P., and Ward, P. 1996. Zooplankton response to a phytoplankton bloom near South Georgia, Antarctica. *Marine Ecology Progress Series*, 144: 195–210.
- Beaugrand, G., McQuatters-Gollop, A., Edwards, M., and Goberville, E. 2013. Long-term responses of North Atlantic calcifying plankton to climate change. *Nature Climate Change*, 3: 263–267.
- Bednaršek, N., Feely, R. A., Reum, J. C. P., Peterson, B., Menkel, J., Alin, S. R., and Hales, B. 2014. *Limacina helicina* shell dissolution as an indicator of declining habitat suitability owing to ocean acidification in the California Current Ecosystem. *Proceedings of the Royal Society B: Biological Sciences*, 281: 20140123.
- Bednaršek, N., Harvey, C. J., Kaplan, I. C., Feely, R. A., and Možina, J. 2016. Pteropods on the edge: Cumulative effects of ocean acidification, warming, and deoxygenation. *Progress in Oceanography*, 145: 1–24.
- Bednaršek, N., Možina, J., Vogt, M., O'Brien, C., and Tarling, G. A. 2012a. The global distribution of pteropods and their contribution to carbonate and carbon biomass in the modern ocean. *Earth System Science Data*, 4: 167–186.
- Bednaršek, N., and Ohman, M. 2015. Changes in pteropod distributions and shell dissolution across a frontal system in the California Current System. *Marine Ecology Progress Series*, 523: 93–103.
- Bednaršek, N., Tarling, G. A., Bakker, D. C. E., Fielding, S., Jones, E. M., Venables, H. J., Ward, P., et al. 2012. Extensive dissolution of live pteropods in the Southern Ocean. *Nature Geoscience*, 5: 881–885.
- Bednaršek, N., Tarling, G. A., Fielding, S., and Bakker, D. C. E. 2012b. Population dynamics and biogeochemical significance of *Limacina helicina antarctica* in the Scotia Sea (Southern Ocean). *Deep Sea Research Part II: Topical Studies in Oceanography*, 59–60: 105–116.
- Bernard, K. S., and Froneman, P. W. 2009. The sub-Antarctic euthecosome pteropod, *Limacina retroversa*: Distribution patterns and trophic role. *Deep Sea Research Part I*, 56: 582–598.
- Comeau, S., Jeffree, R., Teyssie, J. L., and Gattuso, J. P. 2010. Response of the Arctic Pteropod *Limacina helicina* to projected future environmental conditions. *PLoS ONE*, 5: e11362.
- Dadon, J. R., and de Cidre, L. L. 1992. The reproductive cycle of the Thecosomatous pteropod *Limacina retroversa* in the western South Atlantic. *Marine Biology*, 114: 439–442.
- Doubleday, A. J., and Hopcroft, R. R. 2015. Interannual patterns during spring and late summer of larvaceans and pteropods in the coastal Gulf of Alaska, and their relationship to pink salmon survival. *Journal of Plankton Research*, 37: 134–150.
- Fabry, V. J. 1989. Aragonite production by pteropod molluscs in the subarctic Pacific. *Deep Sea Research Part A. Oceanographic Research Papers*, 36: 1735–1751.
- Fabry, V. J. 1990. Shell growth rates of pteropod and heteropod molluscs and aragonite production in the open ocean: implications for the marine carbonate system. *Journal of Marine Research*, 48: 209–222.
- Fabry, V. J., Seibel, B. A., Feely, R. A., and Orr, J. C. 2008. Impacts of ocean acidification on marine fauna and ecosystem processes. *ICES Journal of Marine Science*, 65: 414–432.
- Feely, R. A., Sabine, C. L., Hernandez-Ayon, J. M., Ianson, D., and Hales, B. 2008. Evidence for upwelling of corrosive "acidified" water onto the continental shelf. *Science*, 320: 1490–1492.
- Gannefors, C., Marco, B., Gerhard, K., Martin, G., Ketil, E., Bjorn, G., Haakon, H., et al. 2005. The Arctic sea butterfly *Limacina helicina*: lipids and life strategy. *Marine Biology*, 147: 169–177.
- Harrison, P. J. 2002. Station Papa time series: insights into ecosystem dynamics. *Journal of Oceanography*, 58: 259–264.
- Head, E. J. H., and Pepin, P. 2010. Spatial and inter-decadal variability in plankton abundance and composition in the Northwest Atlantic (1958–2006). *Journal of Plankton Research*, 32: 1633–1648.
- Hodal, M. 2011. Net physical transports, residence times, and new production for Rivers Inlet, British Columbia. Master's thesis, University of British Columbia, Vancouver, BC.

- Hofmann, G. E., and Todgham, A. E. 2010. Living in the now: physiological mechanisms to tolerate a rapidly changing environment. *Annual Review of Physiology*, 72: 127–145.
- Holm-Hansen, O., Naganobu, M., Kawaguchi, S., Kameda, T., Krasovski, I., Tchernyshkov, P., Priddle, J., *et al.* 2004. Factors influencing the distribution, biomass, and productivity of phytoplankton in the Scotia Sea and adjoining waters. *Deep Sea Research Part II: Topical Studies in Oceanography*, 51: 1333–1350.
- Hop, H., Pearson, T., Nøst Hegseth, E., Kovacs, K. M., Wiencke, C., Kwasniewski, S., Eiane, K., *et al.* 2002. The marine ecosystem of Kongsfjorden, Svalbard. *Polar Research*, 21: 42.
- Howes, E. L., Stemann, L., Assailly, C., Irisson, J. O., Dima, M., Bijma, J., and Gattuso, J. P. 2015. Pteropod time series from the North Western Mediterranean (1967–2003): impacts of pH and climate variability. *Marine Ecology Progress Series*, 531: 193–206.
- Hunt, B. P. V., Nelson, R. J., Williams, B., McLaughlin, F. A., Young, K. V., Brown, K. A., Vagle, S., *et al.* 2014. Zooplankton community structure and dynamics in the Arctic Canada Basin during a period of intense environmental change (2004–2009). *Journal of Geophysical Research: Oceans*, 119: 2518–2538.
- Hunt, B. P. V., Pakhomov, E. A., Hosie, G. W., Siegel, V., Ward, P., and Bernard, K. S. 2008. Pteropods in southern ocean ecosystems. *Progress in Oceanography*, 78: 193–221.
- Hunt, B. P. V., Strugnell, J., Bednarsek, N., Linse, K., Nelson, R. J., Pakhomov, E. A., Seibel, B., *et al.* 2010. Poles apart: the “bipolar” pteropod species *Limacina helicina* is genetically distinct. *PLoS ONE*, 5: e9835.
- Jennings, R. M., Bucklin, A., Ossenbrügger, H., and Hopcroft, R. R. 2010. Species diversity of planktonic gastropods (Pteropoda and Heteropoda) from six ocean regions based on DNA barcode analysis. *Deep Sea Research Part II: Topical Studies in Oceanography*, 57: 2199–2210.
- Kobayashi, H. A. 1974. Growth cycle and related vertical distribution of the thecosomatous pteropod *Spiratella* (“*Limacina*”) *helicina* in the central Arctic Ocean. *Marine Biology*, 26: 295–301.
- Lalli, C. M., and Gilmer, R. W. 1989. *Pelagic Snails: The Biology of Holoplanktonic Gastropod Mollusks*. Stanford University Press, Palo Alto, 259 pp.
- Li, W. K. W., McLaughlin, F. A., Lovejoy, C., and Carmack, E. C. 2009. Smallest algae thrive as the Arctic Ocean Freshens. *Science*, 326: 539.
- Lischka, S., Büdenbender, J., Boxhammer, T., and Riebesell, U. 2011. Impact of ocean acidification and elevated temperatures on early juveniles of the polar shelled pteropod *Limacina helicina* mortality, shell degradation, and shell growth. *Biogeosciences*, 8: 919–932.
- Lischka, S., and Riebesell, U. 2012. Synergistic effects of ocean acidification and warming on overwintering pteropods in the Arctic. *Global Change Biology*, 18: 3517–3528.
- Maas, A. E., Elder, L. E., Dierssen, H. M., and Seibel, B. A. 2011. Metabolic response of Antarctic pteropods (Mollusca: Gastropoda) to food deprivation and regional productivity. *Marine Ecology Progress Series*, 441: 129–139.
- Macdonald, P. D. M., and Pitcher, T. J. 1979. Age-groups from size-frequency data: a versatile and efficient method of analyzing distribution mixtures. *Journal of the Fisheries Research Board of Canada*, 36: 987–1001.
- Mackas, D. L., and Galbraith, M. D. 2012. Pteropod time-series from the NE Pacific. *ICES Journal of Marine Science*, 69: 448–459.
- Manno, C., Peck, V. L., and Tarling, G. A. 2016. Pteropod eggs released at high pCO₂ lack resilience to ocean acidification. *Scientific Reports*, 6: 25752.
- McNeil, B. I., and Matear, R. J. 2008. Southern Ocean acidification: a tipping point at 450-ppm atmospheric CO₂. *Proceedings of the National Academy of Sciences*, 105: 18860–18864.
- Moore-Maley, B. L., Allen, S. E., and Ianson, D. 2016. Locally driven interannual variability of near-surface pH and Ω_A in the Strait of Georgia. *Journal of Geophysical Research: Oceans*, 1600–1625.
- Orr, J. C., Fabry, V. J., Aumont, O., Bopp, L., Doney, S. C., Feely, R. A., Gnanadesikan, A., *et al.* 2005. Anthropogenic ocean acidification over the twenty-first century and its impact on calcifying organisms. *Nature*, 437: 681–686.
- Pauly, D. 1998. Why squids, though not fish, can be better understood by pretending they are. *South African Journal of Marine Science*, 20: 47–58.
- Pauly, D. 2013. The ELEFAN system for analysis of length-frequency data from fish and aquatic invertebrate populations. In *ELEFAN in R: a new tool for length-frequency analysis*, pp. 1–25. Ed. by D. Pauly and A. Greenberg, Fisheries Centre Research Reports 21(3). Fisheries Centre, University of British Columbia, Canada.
- Paranjape, M. A. 1968. The egg mass and veligers of *Limacina helicina* Phipps. *Veliger*, 10: 322–326.
- R Core Team 2013. *R: A Language and Environment for Statistical Computing*. R Foundation for Statistical Computing, Vienna.
- Reisdorph, S. C., and Mathis, J. T. 2014. The dynamic controls on carbonate mineral saturation states and ocean acidification in a glacially dominated estuary. *Estuarine, Coastal and Shelf Science*, 144: 8–18.
- Rosenthal, J. J. C., Seibel, B. A., Dymowska, A., and Bezanilla, F. 2009. Trade-off between aerobic capacity and locomotor capability in an Antarctic pteropod. *Proceedings of the National Academy of Sciences*, 106: 6192–6196.
- Schlitzer, R., Ocean Data View, odv.awi.de, 2017.
- Seibel, B. A., and Dierssen, H. M. 2003. Cascading trophic impacts of reduced biomass in the Ross Sea, Antarctica: Just the Tip of the Iceberg? *Biological Bulletin*, 205: 93–97.
- Seibel, B. A., Dymowska, A., and Rosenthal, J. 2007. Metabolic temperature compensation and coevolution of locomotory performance in pteropod molluscs. *Integrative and Comparative Biology*, 47: 880–891.
- Seibel, B. A., Maas, A. E., and Dierssen, H. M. 2012. Energetic plasticity underlies a variable response to Ocean Acidification in the Pteropod, *Limacina helicina antarctica*. *PLoS ONE*, 7: e30464.
- Thabet, A. A., Maas, A. E., Lawson, G. L., and Tarrant, A. M. 2015. Life cycle and early development of the thecosomatous pteropod *Limacina retroversa* in the Gulf of Maine, including the effect of elevated CO₂ levels. *Marine Biology*, 162: 2235–2249.
- Tommasi, D., Hunt, B. P. V., Allen, S. E., Routledge, R., and Pakhomov, E. A. 2014. Variability in the vertical distribution and advective transport of eight mesozooplankton taxa in spring in Rivers Inlet, British Columbia, Canada. *Journal of Plankton Research*, 36: 743–756.
- Tommasi, D., Hunt, B. P., Pakhomov, E. A., and Mackas, D. L. 2013a. Mesozooplankton community seasonal succession and its drivers: Insights from a British Columbia, Canada, fjord. *Journal of Marine Systems*, 115: 10–32.
- Tommasi, D. A., Routledge, R. D., Hunt, B. P. V., and Pakhomov, E. A. 2013b. The seasonal development of the zooplankton community in a British Columbia (Canada) fjord during two years with different spring bloom timing. *Marine Biology Research*, 9: 129–144.
- van der Spoel, S., Dadon, J. R., and Boltovskoy, D. 1999. *South Atlantic Zooplankton*, Backhuys Publishers, Leiden.
- von Bertalanffy, L. 1938. A quantitative theory of organic growth (inquiries on growth laws. II). *Human Biology*, 10: 181–213.

- Wolfe, A. M., Allen, S. E., Hodal, M., Pawlowicz, R., Hunt, B. P. V., and Tommasi, D. 2015. Impact of advection loss due to wind and estuarine circulation on the timing of the spring phytoplankton bloom in a fjord. *ICES Journal of Marine Science*, 73: 1589–1609.
- Yamamoto-Kawai, M., McLaughlin, F. A., Carmack, E. C., Nishino, S., and Shimada, K. 2009. Aragonite undersaturation in the Arctic Ocean: effects of Ocean Acidification and Sea Ice Melt. *Science*, 326: 1098–1100.
- Zhai, L., Platt, T., Tang, C., Sathyendranath, S., and Walne, A. 2013. The response of phytoplankton to climate variability associated with the North Atlantic Oscillation. *Deep Sea Research Part II: Topical Studies in Oceanography*, 93: 159–168.

Handling editor: Rubao Ji